In Situ Surface Chemical Modification of Thin-Film Composite Forward Osmosis Membranes for Enhanced Organic Fouling Resistance

ARTICLE *in* ENVIRONMENTAL SCIENCE & TECHNOLOGY · SEPTEMBER 2013

Impact Factor: 5.33 · DOI: 10.1021/es403179m · Source: PubMed

5 AUTHORS, INCLUDING:

Santiago Romero-Vargas Castrillón
University of Minnesota Twin Cities
17 PUBLICATIONS **440** CITATIONS
SEE PROFILE

Devin Shaffer
Yale University
7 PUBLICATIONS **240** CITATIONS
SEE PROFILE

Jun Ma
Harbin Institute of Technology
319 PUBLICATIONS **4,961** CITATIONS
SEE PROFILE

Menachem Elimelech
Yale University
394 PUBLICATIONS **32,554** CITATIONS
SEE PROFILE

Environmental Science & Technology

Article

pubs.acs.org/est

In Situ Surface Chemical Modification of Thin-Film Composite Forward Osmosis Membranes for Enhanced Organic Fouling Resistance

Xinglin Lu,[†] Santiago Romero-Vargas Castrillón,[‡] Devin L. Shaffer,[‡] Jun Ma,*[,†] and Menachem Elimelech*[,‡]

[†]State Key Laboratory of Urban Water Resource and Environment, Harbin Institute of Technology, Harbin 150090, People's Republic of China

[‡]Department of Chemical and Environmental Engineering, Yale University, New Haven, Connecticut 06520-8286, United States

Supporting Information

ABSTRACT: Forward osmosis (FO) is an emerging membrane-based water separation process with potential applications in a host of environmental and industrial processes. Nevertheless, membrane fouling remains a technical obstacle affecting this technology, increasing operating costs and decreasing membrane life. This work presents the first fabrication of an antifouling thin-film composite (TFC) FO membrane by an in situ technique without postfabrication treatment. The membrane was fabricated and modified in situ, grafting Jeffamine, an amine-terminated poly(ethylene glycol) derivative, to dangling acyl chloride surface groups on the nascent polyamide active layer. Surface characterization by contact angle, Fourier transform infrared spectroscopy (ATR-FTIR), X-ray photoelectron spectroscopy (XPS), zeta potential, atomic force microscopy (AFM), and fluorescence microscopy, confirms the presence of Jeffamine on the membrane surface. We demonstrate the improved fouling resistance of the in situ modified membranes through accelerated dynamic fouling FO experiments using a synthetic wastewater feed solution at high concentration (250 mg/L) of alginate, a model macromolecule for the hydrophilic fraction of wastewater effluent organic matter. Our results show a significantly lower flux decline for the in situ modified membranes compared to pristine polyamide (14.3 ± 2.7% vs 2.8 ± 1.4%, respectively). AFM adhesion force measurements between the membrane and a carboxylate-modified latex particle, a surrogate for the organic (alginate) foulant, show weaker foulant−membrane interactions, further confirming the enhanced fouling resistance of the in situ modified membranes.

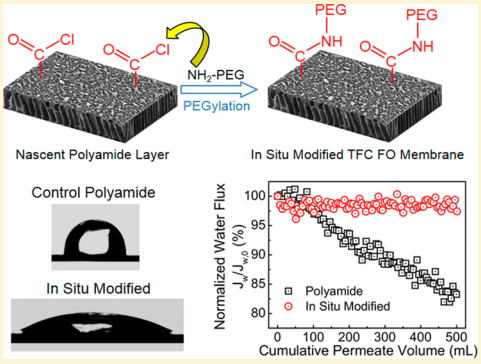

INTRODUCTION

Membrane-based processes hold significant promise in addressing the global challenge of water scarcity.[1] Forward osmosis (FO), an emerging membrane technology that utilizes osmotic pressure to drive water permeation, is the subject of significant current interest,[2,3] due to its potential applications in a variety of environmental and industrial water separation processes that range from wastewater treatment to shale gas produced water purification.[3−9] However, the road toward large-scale FO applications has thus far been hindered by two technical obstacles: lack of high performance membranes tailored to the specific needs of osmosis-driven membrane processes and membrane fouling, particularly for applications involving feed waters without pretreatment.[4,10]

Despite the tremendous success of the thin-film composite (TFC) membrane (comprising a polyamide salt-rejecting active layer and a polysulfone support) in reverse osmosis (RO) seawater desalination,[2,11] its thick and dense support layer renders it inapplicable in FO applications due to internal concentration polarization (ICP).[8] However, recent advances in TFC membrane development have largely addressed this problem, providing the scientific basis for the fabrication of high performance TFC FO membranes.[12−15]

The second technical obstacle faced by FO, which is also an issue in most membrane-based water separation processes, is pervasive membrane fouling that decreases membrane performance. Aromatic polyamide membranes, such as those used in RO and FO, are prone to fouling due to their hydrophobicity, nanoscale morphology, and the presence of negatively charged functional groups.[2,16] The nanoscale "ridge-and-valley" structure characteristic of polyamide active layers may lead to enhanced foulant accumulation on the membrane surface.[17] In addition, negatively charged carboxylate groups on the polyamide surface can promote irreversible binding of natural organic matter through complexation with calcium ions in solution.[2,18]

Received: July 22, 2013
Revised: September 23, 2013
Accepted: September 25, 2013
Published: September 25, 2013

dx.doi.org/10.1021/es403179m | Environ. Sci. Technol. 2013, 47, 12219−12228

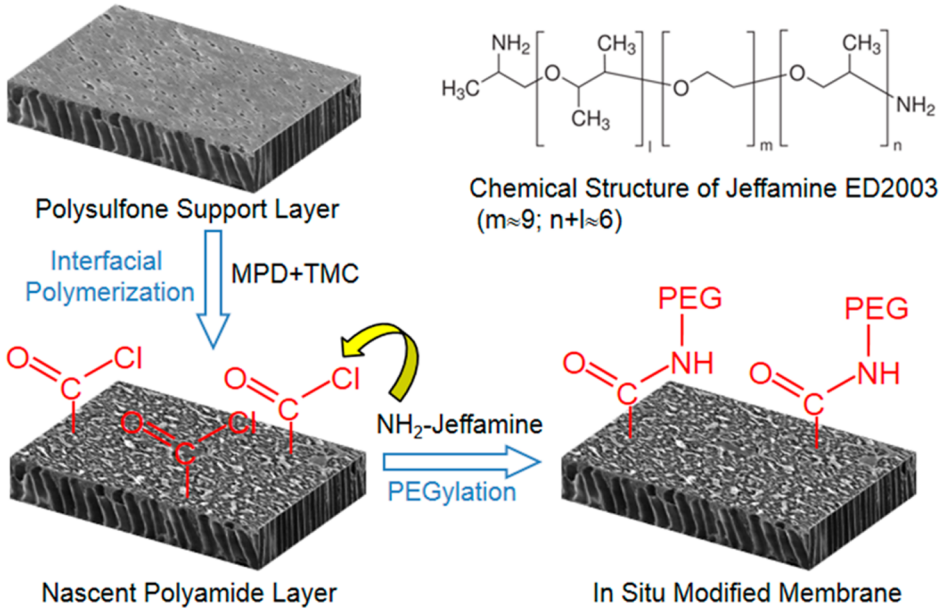

Figure 1. Schematic diagram of the in situ surface modification procedure.

Due to the abundance of organic foulants in natural waters and wastewater effluents, it is virtually impossible to completely eliminate membrane fouling in real applications.[16] However, fouling mitigation, manifested by a lower flux decline and a high extent of flux recovery upon membrane cleaning, is a realizable undertaking that would significantly improve membrane performance and useful life, resulting in savings in energy, operating, and equipment replacement costs. A possible strategy to reduce membrane fouling is surface PEGylation, i.e., attachment of poly(ethylene glycol) (PEG) to the membrane active layer. As shown in numerous studies in the biomedical field,[19] hydrophilic PEG and its derivatives hinder the adsorption of biomolecules on a surface through a combination of entropic repulsion,[20,21] due to compression of the grafted polymer layer, and an enthalpic barrier created by hydration-layer water molecules.[20,22] PEG and its derivatives have also been widely used as the building block of antifouling coatings in TFC RO membranes. Surface PEGylation of RO membranes has been explored by physical adsorption,[23] radical grafting,[24] chemical coupling,[25−27] and plasma polymerization.[28] The modified membranes showed enhanced antifouling properties attributable to higher hydrophilicity, lower surface charge, and the existence of a steric barrier against foulant adsorption.[22,29]

In contrast with the plethora of studies on TFC RO membrane fouling mechanisms and antifouling surface modifications, fouling-resistant TFC FO membranes are not as well studied, with the majority of the fouling literature focusing on commercial asymmetric cellulose acetate FO membranes.[30−34] Among the few studies focusing on FO membrane surface modification, Tiraferri et al.[35,36] reported the fabrication of TFC FO membranes with enhanced antifouling properties by using functionalized superhydrophilic silica nanoparticles. While the study systematically investigated a novel modification protocol, exploring various foulants (bovine serum albumin, natural organic matter, and alginate), experiments were conducted under relatively mild fouling conditions.[35,36] Consequently, there is a definite need to explore alternative pathways toward fouling-resistant FO membranes and to investigate fouling prevention under more exigent experimental conditions, specifically higher foulant concentrations. This is especially relevant to emerging FO processes, such as osmotic dilution[5] and osmotic membrane bioreactors,[6] which operate with high fouling potential feed waters.

This study demonstrates the first fabrication of a TFC FO membrane with enhanced organic fouling resistance by an in situ surface PEGylation without postfabrication treatment. Jeffamine, an amine-terminated poly(ethylene glycol) derivative, is grafted in situ to the nascent polyamide layer by reaction with surface acyl chloride groups during the membrane fabrication process. The fabricated membranes are extensively characterized to confirm the success of the membrane surface modification and to assess its effect on the membrane intrinsic transport properties. We conduct dynamic fouling experiments with alginate as a model organic foulant at previously unexplored high feed concentrations (250 mg/L), resulting in particularly exigent conditions in which to study membrane fouling. Results of our in situ modified TFC FO membranes demonstrate that the extent of fouling is significantly reduced relative to unmodified polyamide membranes. AFM adhesion force measurements provide further insights into the fouling resistance achieved with our modified membranes.

MATERIALS AND METHODS

Materials and Chemicals. Polysulfone (PSf) beads (Mn: 22,000 Da), *N*-*N*-dimethylformamide (DMF, anhydrous, 99.8%), 1-methyl-2-pyrrolidinone (NMP, anhydrous, 99.5%), 1,3-phenylenediamine (MPD, >99%), 1,3,5-benzenetricarbonyl trichloride (TMC, 98%), sodium hypochlorite (NaOCl), and sodium bisulfite ($NaHSO_3$) were used as received (Sigma-Aldrich, St. Louis, MO). A commercial polyester nonwoven fabric (PET, grade 3249, Ahlstrom, Helsinki, Finland) with a thickness of 40 μm was used as a backing layer for the PSf supports. For interfacial polymerization, TMC was dissolved in Isopar-G, a proprietary nonpolar organic solvent (Univar, Redmond, WA). Sodium chloride (NaCl, crystals, ACS reagent) from J.T. Baker (Phillipsburg, NJ) was used in the membrane performance tests. Unless specified, all chemicals

were dissolved in deionized (DI) water obtained from a Milli-Q ultrapure water purification system (Millipore, Billerica, MA).

Thin-Film Composite FO Membrane Fabrication. The pristine (control) TFC membrane was fabricated via interfacial polymerization of MPD and TMC on a hand-cast PSf support. A detailed description of the TFC membrane fabrication is given in previous publications.[12,13]

The PSf support was prepared by nonsolvent induced phase separation. PSf (9 wt %) was dissolved in DMF, stirred for 8 h, and then deaerated in a desiccator for at least 15 h prior to casting. To begin PSf casting, a low-density PET fabric was attached to a clean glass plate using waterproof adhesive tape. NMP was applied to prewet the PET fabric, and the excess NMP was removed using Kimwipes (Kimberly-Clark, Roswell, GA). A casting knife (Gardco, Pompano Beach, FL), set at a gate height of 15 mils (381 μm), was used to spread the PSf solution over the wetted PET fabric. The whole composite was immediately immersed in a precipitation bath containing 3 wt % DMF in DI water at room temperature (23 °C) to initiate the nonsolvent induced phase separation. The PSf support remained in the precipitation bath for 10 min before being transferred to a DI water bath for storage until polyamide formation.

To form the polyamide active layer, the hand-cast PSf supports were first immersed in MPD solution (3.4 wt % in DI water) for 2 min. After removing the excess MPD from the membrane surface using an air knife, the membranes were immersed in the TMC solution (0.15 wt % in Isopar-G) for 1 min to form the polyamide selective layer on the PSf surface, followed by vertical draining of excess TMC solution for 2 min. The membranes were then cured in a DI water bath at 95 °C for 2 min, immersed in NaOCl solution (0.2 g/L, 2 min) followed by immersion in $NaHSO_3$ solution (1 g/L, 30 s), and cured again in DI water at 95 °C for 2 min. The fabricated TFC membranes were rinsed thoroughly and stored in DI water at 4 °C.

In Situ Surface Modification of Thin-Film Composite FO Membrane. The fabrication process of the in situ modified TFC membranes was similar to our TFC membrane fabrication process, with variations adapted from a previous study on reverse osmosis membrane surface modification.[26] A schematic diagram of the in situ modification procedure is presented in Figure 1. After draining the excess TMC solution, the nascent polyamide layer was covered with Jeffamine (ED2003, Mn: 1900 Da, Sigma-Aldrich) solution (1.0 wt % in DI water) for 2 min, resulting in reaction of the primary amine groups at the ends of the Jeffamine molecule with dangling acyl chloride groups on the polyamide surface (Figure 1). With the exception of this surface modification step, the fabrication procedure of the in situ modified membranes is analogous to that of the control polyamide membranes.

Evaluation of Membrane Intrinsic Properties. Pure water permeability, A, solute permeability, B, and solute rejection, R, of the membranes were determined in a laboratory-scale crossflow RO unit.[37] Following characterization in the RO unit, the same membrane sample was characterized in an FO unit (with the active layer facing the feed solution) to determine the support layer structural parameter, S.[38] The details of the membrane characterization methods can be found in the Supporting Information (SI).

Surface Characterization of In Situ Modified Thin-Film Composite FO Membrane. Surface hydrophilicity of the membranes was evaluated by measuring the contact angle of DI water using the sessile drop method. A 1-μL droplet was placed on the air-dried membrane surface, and photographed using a digital camera. The contact angles of the left and right sides of the droplet were determined using a computer program (VCA, Optima XE, AST Products, Billerica, MA). To account for variations in the measurements, we performed eight measurements on each sample. Three independently cast membranes of each type were thus characterized.

Fourier transform infrared spectroscopy (FTIR) was used to confirm Jeffamine grafting to the active layer of the modified membranes. The FTIR spectrometer (Nicolet 6700, Thermo Scientific) was equipped with an attenuated total reflectance (ATR) accessory comprising a ZnSe crystal and a pressure gripper device to achieve intimate contact between the ATR crystal and the membrane sample. Measurements were carried out in the mid-IR region (4000 to 800 cm^{-1}) at a spectrum resolution of 0.482 cm^{-1}, using 64 scans for both the background and sample.

The membranes were also characterized by X-ray photoelectron spectroscopy (XPS) for elemental composition, zeta potential for charge characteristics, atomic force microscopy (AFM) for surface morphology, and fluorescence microscopy to confirm the presence of Jeffamine on the modified membrane surface. The relevant experimental methods can be found in the SI.

Model Foulant and Solution Chemistry. Sodium alginate (Sigma-Aldrich, St. Louis, MO), a polysaccharide, was chosen as a model organic foulant. As per manufacturer's specifications, the molecular weight of sodium alginate ranges from 12 to 80 kDa. A stock solution (10 g/L) was made by dissolving the sodium alginate dry powder in DI water and stored in a sterilized bottle at 4 °C. The synthetic wastewater, simulating typical secondary wastewater effluents from selected wastewater treatment plants in California,[36,39] was prepared by dissolving 0.45 mM KH_2PO_4, 9.20 mM NaCl, 0.61 mM $MgSO_4$, 0.5 mM $NaHCO_3$, 0.5 mM $CaCl_2$, and 0.93 mM NH_4Cl, in DI water. The pH of the feed solution was adjusted to 7.4. The feed solution calculated ionic strength is 14.9 mM (Visual MINTEQ 3.0).

FO Fouling Experiments. A laboratory-scale crossflow FO unit was used in the FO fouling experiments. The experiments were conducted at cocurrent crossflows of 8.5 cm/s for both draw and feed channels without spacers, and at 25 ± 0.5 °C. The protocol for all the fouling experiments comprised the following steps. First, a clean membrane sample was loaded into the FO cell with the active layer facing the feed solution (FO mode). The system was stabilized with DI water on both feed and draw sides. Next, aliquots of inorganic stock solutions were added to the feed solution to prepare the synthetic wastewater with the above-mentioned composition. The draw solution was supplemented with 2−4 M NaCl in order to reach an initial water flux of 20 L m^{-2} h^{-1}. After the flux became stable, 250 mg/L of alginate was added to the feed solution to begin the accelerated fouling experiment. The experiments were conducted for 15−20 h, until a cumulative permeate volume of 500 mL was collected. Water flux throughout the experiment was monitored by a computer at 1 min intervals. Given that our goal is to investigate membrane fouling, the water flux data presented herein have been corrected to eliminate the contribution to the flux decrease due to draw solution dilution. Therefore, the data shown reflect the flux decrease due solely to membrane fouling. The data analysis methodology can be found in the SI.

Physical cleaning experiments were conducted immediately following the FO fouling runs, with a foulant-free solution (15 mM NaCl) circulated through the feed and draw compartments for 15 min at a crossflow velocity of 21.4 cm/s. Following cleaning, the cleaned membrane water flux was measured again following the same experimental protocol as described for the baseline experiment.

AFM Adhesion Force Measurements. Adhesion force measurements were performed in a multimode AFM operating in contact mode, following the protocol developed by Li and Elimelech.[40] A 4.0-μm carboxyl-modified latex particle (CML, carboxyl content 19.5 μEq/g, Life Technologies, Eugene, OR) was glued to the tip of a SiN cantilever (Bruker NP-O10, Santa Barbara, CA, spring constant of 0.06 N/m) using optical adhesive, and subsequently cured for 20 min in a UV cleaner. All measurements were performed in a liquid cell filled with ~2 mL of synthetic wastewater with the same composition as indicated above. The cantilever deflection sensitivity was calibrated on a glass surface by measuring the slope of the deflection during piezoelectric stage retraction. Membrane adhesion forces were determined by converting the deflection vs piezo retraction data to force vs particle-membrane separation applying Hooke's law.[41] At least 125 retraction events were recorded for every sample distributed over 5 randomly chosen locations on the membrane surface.

RESULTS AND DISCUSSION

Membrane Surface Characteristics. The modified membrane surface was extensively characterized to confirm the success of the Jeffamine grafting and to study the effect of the in situ chemical modification on the membrane surface characteristics.

Figure 2 presents the average contact angle of DI water on the surface of control and modified membranes. The control

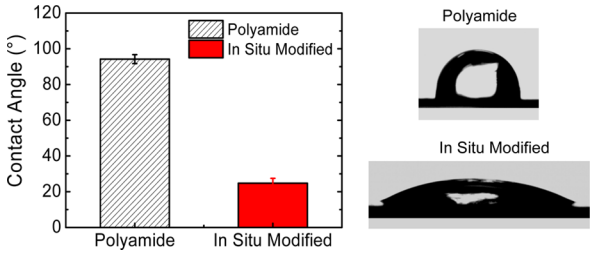

Figure 2. Contact angle of a sessile DI water droplet (1 μL) on the membrane surface for control polyamide and in situ modified membranes. Eight contact angle measurements on random locations in each sample were performed with DI water at room temperature (23 °C), and at unadjusted pH (~5.7). Values reported are averages of the measurements performed in three independently cast membranes of each type. Representative pictures of DI water droplets are also included.

polyamide membrane has a contact angle of 94.2 ± 2.5°, which is consistent with previously published data on hand-cast polyamide membranes.[35] The wettability of a solid surface, indicated by the contact angle, is mainly determined by the microstructure and the chemical composition of the surface.[42] The higher surface roughness of our hand-cast polyamide membranes results in a less wettable membrane surface and high contact angle because air bubbles become trapped between the water droplet and the membrane due to its ridge-and-valley structure.[35,43] In addition, aromatic rings are the dominant functional groups in polyamide; these entities cannot form hydrogen bonds with water and therefore contribute to the high contact angle observed in the control membranes.[44] The modified membrane exhibits a significantly lower contact angle of 24.8 ± 2.7°, evidencing a more hydrophilic surface due to the grafted Jeffamine chains.

The presence of Jeffamine on the membrane surface was also verified using ATR-FTIR. The ATR-FTIR spectra of both control and modified membranes are presented in Figure S1 of the SI. The modified membrane spectrum exhibits a clear peak at 2875 cm^{-1}. This peak, which is not observed in the control membrane spectrum, is due to the CH_2 symmetric stretch of ethylene glycol and propylene glycol monomers, and indicates successful Jeffamine grafting.[45] However, both membranes show peaks at 1080, 1105, 1150, and 1170 cm^{-1}, ascribed to the C═C stretch of aromatic rings,[25,45] as well as peaks at 1660 and 1544 cm^{-1} due to the amide I and amide II modes,[46] and peaks due to the underlying polysulfone support at 1243 and 1584 cm^{-1}.[27] The ether groups in ethylene and propylene glycol monomers of the Jeffamine chain show a peak at 1080 cm^{-1}, corresponding to the C−O and C−C bond stretch.[45] Because of the abundance of the C−O bonds in Jeffamine, we expect an increase in absorbance at 1080 cm^{-1} in the in situ modified membrane spectrum relative to the aromatic peaks of the native polyamide, which should exhibit no systematic increase in absorbance upon grafting.

In order to investigate this phenomenon, we computed the degree of grafting (DG) from the ATR-FTIR spectra. DG is defined as follows:[47,48]

$$\mathrm{DG} = \frac{I_{\mathrm{PEG}}}{I_{\mathrm{aromatic}}} \quad (1)$$

where I_{PEG} is the absorbance at 1080 cm^{-1}, corresponding to the C−O and C−C bond stretching of PEG, and C═C stretch of underlying aromatic rings,[26] and I_{aromatic} is the absorbance at either 1150 or 1170 cm^{-1}, solely ascribed to the C═C stretch of aromatic rings.[45] The absorption bands at 1150 or 1170 cm^{-1}, being part of the native polyamide active layer, are an appropriate normalization factor, since they change insignificantly when the grafted polymer layer is smaller than the penetration depth of the IR wave (about 1 μm),[47] as is the case for the PEG-like polymers (molecular weight 1900 g/mol, radius of gyration ≈ 1.5 nm[49,50]) considered in this study. As expected, the modified membrane shows higher DG values relative to both 1150 and 1170 cm^{-1} (Figure 3), indicating an increase of the absorbance at 1080 cm^{-1} after Jeffamine modification. It should be noted that our definition of DG implies that this quantity has a finite value for the control membranes. We emphasize that this is due to the absorption band of pristine polyamide at 1080 cm^{-1}. The data in Figure 3 provide further evidence of the successful grafting of Jeffamine on the membrane surface.

XPS was also performed to analyze the surface elemental composition. Previous studies using chemically grafted polymers have reported an increase in the oxygen surface content upon membrane modification.[25−27] On the basis of its chemical structure (Figure 1), the O/C ratio of Jeffamine (0.341−0.468) is higher than that of the carboxylated polyamide surface (0.167−0.267);[51] a higher oxygen surface content is therefore expected in the modified membranes, and was indeed observed. The oxygen-to-carbon (O/C) ratio determined by XPS (Table 1), shows a ~9% increase in the

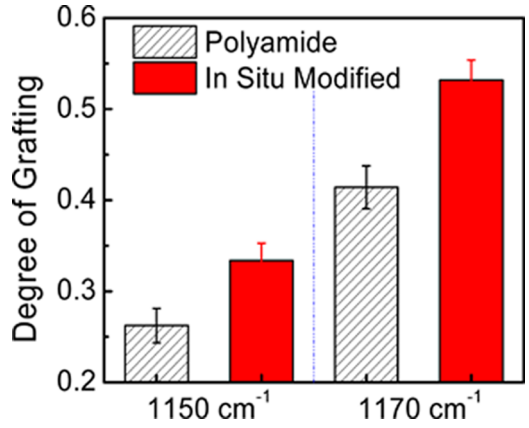

Figure 3. Degree of grafting (DG) for control polyamide (black patterned) and in situ modified membranes (red solid), computed from ATR-FTIR spectra relative to aromatic absorption bands at 1150 cm^{-1} and 1170 cm^{-1}.

Table 1. Surface Characteristics of Control Polyamide and In Situ Modified FO Membranes

	polyamide	in situ modified
XPS relative O/C ratio	0.281 ± 0.004	0.305 ± 0.010
ζ potential[a] (mV)	−16.0	−5.5
	surface roughness	
R_{rms}[b] (nm)	139 ± 13	90 ± 9
R_a[c] (nm)	109 ± 10	73 ± 8
R_{max}[d] (nm)	1187 ± 273	668 ± 208
SAD[e] (%)	43.0 ± 11.7	37.4 ± 16.4

[a]Solution chemistry for the ζ potential measurements: 1 mM KCl at pH 7.4. [b]Root mean squared roughness (R_{rms}): the RMS deviation of the peaks and valleys from the mean plane. [c]Average roughness (R_a): arithmetic average of the absolute values of the surface height deviations measured from the mean plane. [d]Maximum roughness (R_{max}): the maximum vertical distance between the highest and lowest data points in the image following the plane fit. [e]Surface area difference (SAD): the increase in surface area (due to roughness) over a perfectly flat plane with the same projected area.

modified membrane O/C ratio relative to the control polyamide membrane.

The zeta (ζ) potential at the pH of our synthetic wastewater solution (pH 7.4) is summarized in Table 1 for the control and modified membranes. Similarly, the variation of zeta potential with pH over the pH range 4−9 is given in Figure S2 of the SI. During the fabrication process of the control polyamide membrane, unreacted acyl chloride groups in the nascent polyamide layer are hydrolyzed to form carboxyl groups after the TFC membrane is immersed in water.[52,53] At pH $\lesssim$ 5, surface carboxyl groups are uncharged, while surface primary amine groups become protonated. We surmise that the positive zeta potential observed at pH < 5 in the control membrane, is due to the combination of protonated carboxyl and amine groups. As the pH is increased above the pK_a of the carboxyl groups, which is around 5.2,[54] carboxyl group deprotonation dominates the surface charge of the membrane,[35] resulting in a negative zeta potential on the control polyamide membrane surface (Figure S2 of the SI).

For the modified membrane, the zeta potential at pH $\gtrsim$ 5 is less negative compared with that of the control polyamide membrane. We offer two possible explanations. First, the covalent bonding between the nascent acyl chloride groups and the amine-terminated Jeffamine molecules results in a decrease of the carboxyl group surface density, thus imparting a less negative surface charge to the modified membrane surface. Another possible explanation is the protonation of the grafted Jeffamine. Jeffamine has a pK_a of 7.1,[55] which is higher than that of surface carboxyl groups.[54] This could also lead to a less negatively charged surface on the modified membrane.

Membrane surface roughness was characterized by AFM. Representative three-dimensional images of the membranes are presented in the SI (Figure S3), and the calculated results are summarized in Table 1. The control membrane shows the ridge-and-valley surface morphology (Figure S3a of the SI) characteristic of TFC polyamide membranes.[2,52] The RMS, average, and maximum surface roughness of the control polyamide membrane (R_{rms} = 139 ± 13 nm, R_a = 109 ± 10 nm, and R_{max} = 1187 ± 273 nm) and the surface area difference (SAD) of 43.0 ± 11.7%, are consistent with previously published data.[35] The three-dimensional image of the Jeffamine-modified membrane shows morphological features that are similar to those of the control (Figure S3b of the SI), although the ridge-and-valley morphology appears to be less pronounced. Accordingly, the modified membrane has lower values of R_{rms}, R_a, R_{max}, and SAD, indicating lower surface roughness.

Previous studies have arrived at different conclusions concerning the effect of surface modification with PEG on TFC polyamide membrane morphology. Kang et al.[26] and Van Wagner et al.[25] observed an increase in surface roughness after modification, while other groups reported a decrease.[23,56] Due to differences in the modification methods and molecular weight of the grafted polymer, it is difficult to make a direct comparison of previous works with ours. For our modification method, the decrease could be attributed to the relatively higher surface roughness of the pristine hand-cast polyamide.[17,25] We propose that Jeffamine molecules penetrate into the valley regions of the TFC polyamide layer, thus resulting in a morphologically smoother membrane surface. As we discuss later, previous studies suggest a decrease in the fouling propensity of TFC membranes with decreased surface roughness.[17]

Fluorescence labeling has been extensively used in biology.[57] We apply this technique to confirm the presence of Jeffamine on the modified membrane surface. By controlling the molar ratio of the reactants (as described in the SI), one of the two terminal amine groups of the Jeffamine chain can be labeled with Rhodamine B isothiocyanate, a fluorescent dye, leaving the other amine group available for in situ surface modification. The fluorescence images of the control and modified membranes are presented in Figure S4 of the SI. Compared with the control polyamide membrane (Figure S4a of the SI), strong red fluorescence is observed on the modified membrane surface (Figure S4b of the SI), indicating the successful grafting of Rhodamine B isothiocyanate-labeled Jeffamine.

Membrane Intrinsic Properties. Because Jeffamine is only grafted onto the membrane active layer, the structural parameter, S, which is an intrinsic property of the PSf support layer, did not change after modification (804 ± 150 μm vs 749 ± 166 μm for the control and modified membranes, respectively) as seen in Figure S5 of the SI. Similarly, the salt permeability, B, of the modified membranes (0.39 ± 0.23 L m^{-2} h^{-1}) is roughly the same as that of the control (0.43 ± 0.10 L m^{-2} h^{-1}), as is the observed salt rejection, R (98.25 ± 0.60% vs 98.27 ± 0.21% for the control and modified membranes,

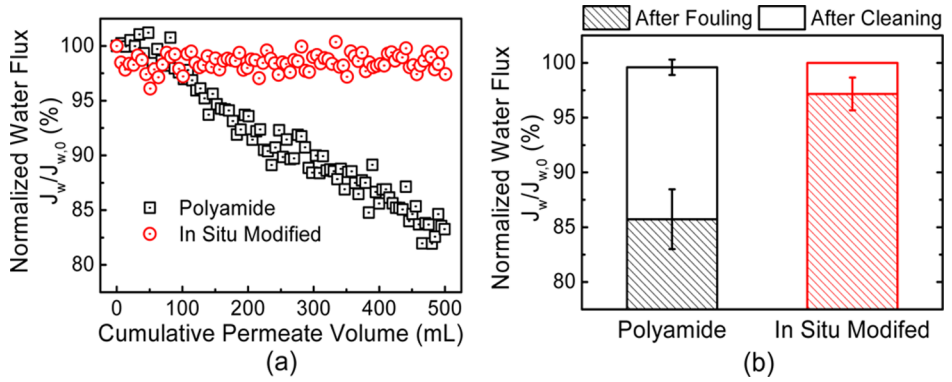

Figure 4. (a) Representative fouling curves for the control polyamide membranes and the in situ modified membranes. Fouling conditions were as follows: the feed solution as described in the Materials and Methods section supplemented with 250 mg/L of alginate as model organic foulant, at pH 7.4; the draw solution consisted of NaCl at 2−4 M concentration, resulting in an initial permeate water flux of ∼20 L m^{-2} h^{-1}. The system temperature was maintained at 25 ± 0.5 °C, and the crossflow velocity of the feed and draw streams was set to 8.5 cm/s. After the fouling run, the system was cleaned by circulating 15 mM NaCl solution for 15 min at a crossflow velocity of 21.4 cm/s through the feed and draw solution compartments. To reduce experimental noise, data were smoothed using a 5-point window moving average. (b) Summarized forward osmosis organic fouling results of triplicate experiments with control polyamide (black) and in situ modified (red) membranes. The percentage of water flux recovered after the physical cleaning step is shown as blank columns.

respectively). These observations imply that the in situ modification procedure is a nondestructive method and will not cause detrimental defects on the selectivity of the polyamide layer surface. However, the water permeability coefficient, *A*, of the modified membranes (0.89 ± 0.08 L m^{-2} h^{-1} bar^{-1}) is significantly lower than that of the control (1.71 ± 0.14 L m^{-2} h^{-1} bar^{-1}). This could be attributed to the grafted Jeffamine layer on the surface, which increases the resistance to transport of water molecules across the active layer.[58] Further optimization of the modification experimental conditions,[59] including PEG concentration, molecular weight, and contact time, could be performed in order to strike a balance between fouling resistance and membrane performance.

Dynamic Fouling with Alginate. Dynamic fouling experiments were conducted to evaluate the fouling propensity of control and modified membranes. We considered alginate as a surrogate for polysaccharides, the main constituents of extracellular polymeric substances (EPS), whose presence in wastewater effluents leads to membrane fouling.[60,61] Polysaccharides are common at concentrations around 33 mg/L in wastewater effluents.[62] We chose to conduct our experiments at significantly higher alginate concentrations (250 mg/L) in order to test our modified membranes under particularly exigent experimental conditions, and to observe fouling within a shorter time scale of ∼18 h.

The dependence of water flux on the cumulative permeate volume recorded during fouling experiments is presented in Figure 4a for control and modified membranes. The flux after permeation of 500 mL, normalized by the initial water flux, is presented in Figure 4b as patterned bars, while the recovered flux after physical cleaning is shown as blank columns.

As a consequence of membrane fouling, the control polyamide membranes exhibit a decrease in permeate water flux of 14.3 ± 2.7% over the course of the experimental run, compared to 2.8 ± 1.4% for the modified membranes. Previous studies have shown that Ca^{2+} ions (0.5 mM) in the synthetic wastewater feed can act as "bridges" between alginate molecules, leading to the formation of a cross-linked alginate gel layer on the membrane surface.[30,36] This gel layer increases the hydraulic resistance to water transport, thus causing a decrease of the water flux.[58] At the same time, the gel layer also hinders the back diffusion of ions retained by the membrane active layer and those permeating from the draw solution through the active layer, resulting in salt accumulation within the alginate fouling layer, and consequently, a decrease in the osmotic pressure difference. This phenomenon, known as cake enhanced osmotic pressure (CEOP), can lead to a significant flux decline in RO[63] as well as FO.[10,64]

Compared with the control polyamide membranes, the modified membrane exhibits a lower flux decline (Figure 4b) and thus improved fouling resistance. The interplay of surface wettability, steric hindrance, and surface electrostatic interactions is responsible for the observed fouling resistance. First, the grafted Jeffamine molecules impose a steric barrier against the adsorption of the alginate molecules.[27] Second, the reaction between the nascent acyl chloride groups and the amine-terminated Jeffamine molecules results in a decrease of the number of surface carboxyl groups that can act as complexation sites for alginate in the presence of Ca^{2+}, thus improving the antifouling properties of the modified membrane.[18] Third, the presence of Jeffamine, containing hydrophilic monomers, increases the hydrophilicity of the membrane surface (Figure 2). The abundance of oxygen atoms as hydrogen bond acceptors in ethylene glycol and propylene glycol monomers leads to a hydration layer of water molecules that hinders alginate adsorption.[36] Lastly, the enhanced fouling resistance can also be attributed to a decrease in surface roughness. A smoother surface can potentially avoid the accumulation of alginate molecules on the polyamide.[17] Moreover, permeation across a low-roughness active layer may result in a more spatially uniform flux distribution and, consequently, fewer regions with locally high water fluxes (hence prone to fouling).[65]

The fouling phenomena described above can be explained by a combination of foulant−membrane and foulant−foulant interactions that dominate at different stages of the experiment. Foulant−membrane interactions dominate initially, leading to adhesion of foulant molecules on the active layer.[31,36] The absence of a hydraulic pressure difference in FO operations leads to a small amount of alginate adsorption on the membrane surface, which is not sufficient to cause a significant water flux decline. As shown in Figure 4a, the flux across the

control polyamide membrane does not appear to decrease within the first 75 mL of permeation. However, flux decline becomes evident (at permeate volumes > ~100 mL) as alginate continues to accumulate on the membrane surface, forming a continuous foulant layer that increases the hydraulic resistance and CEOP. At this and the latter stages of control membrane fouling, with further bridging occurring between the alginate film on the surface and alginate molecules in solution, foulant–foulant interactions, leading to a foulant layer that spans the membrane active layer, determine the extent of membrane fouling.[31] For the modified membrane, however, the flux remains stable throughout the experiment (Figure 4a) or exhibits a less pronounced decrease (Figure 4b), suggesting that a thinner and/or discontinuous alginate layer is present on the modified surface. Therefore, foulant–membrane interactions, which are weakened by the grafted Jeffamine layer, appear to be the determining factor of alginate fouling. The formation of an initial alginate layer is the necessary first step in alginate membrane fouling; absent this precursor layer, as observed with the modified membranes, foulant–foulant interactions leading to foulant layer growth cannot take place, and the extent of fouling is significantly reduced.

To assess the reversibility of alginate fouling, cleaning experiments were conducted immediately following the fouling experiments for each membrane sample. As shown in Figure 4b, the water flux is almost completely recovered for both control and modified membranes, in agreement with previous work.[36] Compared with pressure-driven membrane processes, including RO and nanofiltration (NF), the absence of hydraulic pressure in FO results in a loosely adsorbed foulant layer that can be easily sheared off by simple physical cleaning.[31]

Relating Fouling Behavior to Foulant–Membrane Interactions. AFM adhesion force measurements were carried out to assess the intrinsic fouling propensity of membrane surfaces in the absence of water permeation. As a substitute for alginate, we employed a cantilever functionalized with a carboxyl-modified latex (CML, 4 μm in diameter) particle. The surface chemistry of the CML particle, rich in carboxyl groups, renders it an appropriate surrogate for alginate macromolecules.[18,36,40]

Figure 5 presents histograms summarizing the adhesion force measurements of control polyamide and in situ modified membranes. The histograms were constructed from 125 retraction events (126 for the modified), recorded over 5 random locations on each membrane active layer. The data are presented as a function of the maximum (in absolute value) adhesion force normalized by the radius of the AFM particle probe. Within the Derjaguin approximation, this quantity is proportional to the adhesion interaction energy per unit surface area.[66]

Figure 5 (lower panel) shows that the distribution of probe–membrane adhesion forces of the modified membrane is generally shifted to the right-hand side (i.e., low adhesion forces) compared with that of the control polyamide membrane (Figure 5, upper panel). We observe that the distribution of probe–control membrane adhesion forces can be well described by a log-normal distribution centered around −0.5 mN/m (note the log-normal function fitted to the control data in Figure 5). However, adhesion forces of the modified membrane are distributed bimodally, being described as the sum of a weakly interacting population with a mean of −0.15 mN/m and a more strongly interacting population with a mean adhesion force of −1.0 mN/m. Accordingly, Figure 5 shows

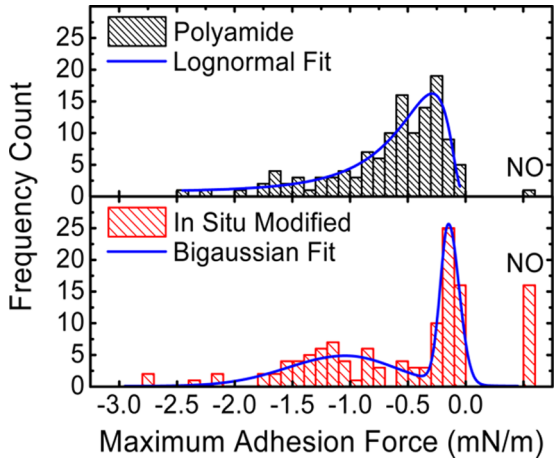

Figure 5. Distribution of colloidal probe–membrane adhesion forces of control polyamide and in situ modified membrane active layer surfaces. Measurements were performed by contact mode AFM at room temperature in a liquid cell filled with synthetic wastewater (pH 7.4) of the following composition: 0.45 mM KH_2PO_4, 9.2 mM NaCl, 0.61 mM $MgSO_4$, 0.5 mM $NaHCO_3$, 0.5 mM $CaCl_2$, and 0.93 mM NH_4Cl. At least 125 retraction measurements distributed over five randomly chosen locations were performed for each sample. The columns labeled "NO" indicate the fraction of the population of force measurements in which no adhesion was observed.

that, for the modified membrane, a bigaussian function adequately describes the probe–membrane adhesion force distribution. The weakly interacting population (i.e., that characterized by absolute values of adhesion forces <0.25 mN/m) constitutes 53% of the measured events. Similarly, for the control surface, the fraction of events exhibiting forces with absolute values <0.25 mN/m represents 27% of the total population. Also noteworthy is the fact that a visible fraction of the force measurements performed on the modified membrane exhibited no measurable adhesion forces (note the "NO" column in Figure 5). In this case, no measurable interaction well was detected, indicating that repulsive probe–membrane interactions predominate. Conversely, only one no-adhesion event was recorded in measurements with the control polyamide surface. We note that we classified as no-adhesion events those force curves in which the adhesion force (normalized by the probe radius) was less than 0.05 mN/m or whenever an interaction force less than 0.1 mN/m was associated with a rupture distance (i.e., the separation at which the force vanishes to zero) greater than 300 nm. In both instances, the interaction forces were weak and could not be clearly distinguished from the noise associated with the retraction baseline.

Despite the fact that the force distribution of the modified membrane exhibits a peak characteristic of high interaction forces (note the secondary peak centered at −1.0 mN/m in Figure 5 for the modified membrane), the presence of a significant peak of weak probe–membrane interaction forces of the modified membrane, together with the observation of no-adhesion events, constitutes further evidence of the lower fouling propensity of the modified membranes compared to the control polyamide.

Environmental Implications. We have demonstrated the fabrication of FO membranes whose enhanced fouling resistance permits operation at high water fluxes over extended periods of time. Membrane materials such as those presented

herein could find applications in osmosis-driven processes that expose the membrane selective layer to feed waters with high foulant concentrations, and where circumventing feed pretreatment is desirable for practical and economic reasons. These applications include seawater dilution for RO desalination,[4] osmotic dilution of RO brines,[5] osmotic membrane enclosures for algae growth,[4] and osmotic membrane bioreactors for wastewater reclamation.[6] Given the significant current and future interest in the exploration of shale gas extraction sites, fouling resistant FO membranes could also find applications in treatment and reuse of produced water, which typically contains high levels of salts and organic matter.[9]

■ ASSOCIATED CONTENT

Supporting Information

Details on the characterization of membrane transport properties (S1); surface characterization protocols (XPS, zeta potential, AFM, and fluorescence labeling) (S2); and flux data analysis methodology (S3); ATR-FTIR spectra of control polyamide and in situ modified membranes (Figure S1); active layer zeta potentials of control polyamide and in situ modified membranes as a function of solution pH (Figure S2); AFM images of control polyamide and in situ modified membranes (Figure S3); fluorescence images of control polyamide and in situ modified membranes labeled with Rhodamine B-Jeffamine (Figure S4); transport parameters of control polyamide and in situ modified membranes (Figure S5). This material is available free of charge via the Internet at http://pubs.acs.org.

■ AUTHOR INFORMATION

Corresponding Author

*Tel: +86 451 86283010 (J.M.); +1 203 432 2789 (M.E.). Fax: +86 451 86283010 (J.M.); +1 203 432 4387 (M.E.). E-mail: majun@hit.edu.cn (J.M.); menachem.elimelech@yale.edu (M.E.).

Notes

The authors declare no competing financial interest.

■ ACKNOWLEDGMENTS

Financial support from the Department of Defense through the Strategic Environmental Research and Development Program (SERDP, Project No. 12 ER01-054/ER-2217) and the National Science and Technology Pillar Program of China (No. 2012BAC05B02) is gratefully acknowledged. We thank Dr. Genggeng Qi (Cornell University) for performing the XPS analysis of our membrane samples, Dr. Yunxia Hu (Yale University) for help with the fluorescence labeling technique, and Dr. Alberto Tiraferri (University of Geneva) for useful discussions on Atomic Force Microscopy. We also acknowledge a graduate fellowship (to X.L.) made possible by China Scholarship Council, the use of facilities supported by YINQE, and NSF MRSEC DMR 1119826.

■ REFERENCES

(1) Shannon, M. A.; Bohn, P. W.; Elimelech, M.; Georgiadis, J. G.; Marinas, B. J.; Mayes, A. M. Science and technology for water purification in the coming decades. *Nature* **2008**, *452* (7185), 301–310.

(2) Elimelech, M.; Phillip, W. A. The future of seawater desalination: energy, technology, and the environment. *Science* **2011**, *333* (6043), 712–717.

(3) McGinnis, R. L.; Elimelech, M. Global challenges in energy and water supply: The promise of engineered osmosis. *Environ. Sci. Technol.* **2008**, *42* (23), 8625–8629.

(4) Hoover, L. A.; Phillip, W. A.; Tiraferri, A.; Yip, N. Y.; Elimelech, M. Forward with osmosis: Emerging applications for greater sustainability. *Environ. Sci. Technol.* **2011**, *45* (23), 9824–30.

(5) Cath, T. Y.; Hancock, N. T.; Lundin, C. D.; Hoppe-Jones, C.; Drewes, J. E. A multi-barrier osmotic dilution process for simultaneous desalination and purification of impaired water. *J. Membr. Sci.* **2010**, *362* (1–2), 417–426.

(6) Achilli, A.; Cath, T. Y.; Marchand, E. A.; Childress, A. E. The forward osmosis membrane bioreactor: A low fouling alternative to MBR processes. *Desalination* **2009**, *239* (1–3), 10–21.

(7) Zhang, F.; Brastad, K. S.; He, Z. Integrating forward osmosis into microbial fuel cells for wastewater treatment, water extraction and bioelectricity generation. *Environ. Sci. Technol.* **2011**, *45* (15), 6690–6696.

(8) Cath, T. Y.; Childress, A. E.; Elimelech, M. Forward osmosis: Principles, applications, and recent developments. *J. Membr. Sci.* **2006**, *281* (1–2), 70–87.

(9) McGinnis, R. L.; Hancock, N. T.; Nowosielski-Slepowron, M. S.; McGurgan, G. D. Pilot demonstration of the NH_3/CO_2 forward osmosis desalination process on high salinity brines. *Desalination* **2013**, *312*, 67–74.

(10) Boo, C.; Elimelech, M.; Hong, S. Fouling control in a forward osmosis process integrating seawater desalination and wastewater reclamation. *J. Membr. Sci.* **2013**, *444*, 148–156.

(11) Cadotte, J.; Petersen, R.; Larson, R.; Erickson, E. A new thin-film composite seawater reverse osmosis membrane. *Desalination* **1980**, *32*, 25–31.

(12) Yip, N. Y.; Tiraferri, A.; Phillip, W. A.; Schiffman, J. D.; Elimelech, M. High performance thin-film composite forward osmosis membrane. *Environ. Sci. Technol.* **2010**, *44* (10), 3812–3818.

(13) Tiraferri, A.; Yip, N. Y.; Phillip, W. A.; Schiffman, J. D.; Elimelech, M. Relating performance of thin-film composite forward osmosis membranes to support layer formation and structure. *J. Membr. Sci.* **2011**, *367* (1–2), 340–352.

(14) Wei, J.; Qiu, C.; Tang, C. Y.; Wang, R.; Fane, A. G. Synthesis and characterization of flat-sheet thin film composite forward osmosis membranes. *J. Membr. Sci.* **2011**, *372* (1–2), 292–302.

(15) Wang, R.; Shi, L.; Tang, C. Y.; Chou, S.; Qiu, C.; Fane, A. G. Characterization of novel forward osmosis hollow fiber membranes. *J. Membr. Sci.* **2010**, *355* (1–2), 158–167.

(16) Rana, D.; Matsuura, T. Surface modifications for antifouling membranes. *Chem. Rev.* **2010**, *110* (4), 2448–2471.

(17) Vrijenhoek, E. M.; Hong, S.; Elimelech, M. Influence of membrane surface properties on initial rate of colloidal fouling of reverse osmosis and nanofiltration membranes. *J. Membr. Sci.* **2001**, *188* (1), 115–128.

(18) Mo, Y.; Tiraferri, A.; Yip, N. Y.; Adout, A.; Huang, X.; Elimelech, M. Improved antifouling properties of polyamide nanofiltration membranes by reducing the density of surface carboxyl groups. *Environ. Sci. Technol.* **2012**, *46* (24), 13253–61.

(19) Harris, J. M.; Chess, R. B. Effect of pegylation on pharmaceuticals. *Nat. Rev. Drug Discovery* **2003**, *2* (3), 214–221.

(20) Israelachvili, J.; Wennerstrom, H. Role of hydration and water structure in biological and colloidal interactions. *Nature* **1996**, *379* (6562), 219–225.

(21) Morra, M. On the molecular basis of fouling resistance. *J. Biomater. Sci., Polym. Ed.* **2000**, *11* (6), 547–569.

(22) Ostuni, E.; Chapman, R. G.; Holmlin, R. E.; Takayama, S.; Whitesides, G. M. A survey of structure-property relationships of surfaces that resist the adsorption of protein. *Langmuir* **2001**, *17* (18), 5605–5620.

(23) Louie, J. S.; Pinnau, I.; Ciobanu, I.; Ishida, K. P.; Ng, A.; Reinhard, M. Effects of polyether-polyamide block copolymer coating on performance and fouling of reverse osmosis membranes. *J. Membr. Sci.* **2006**, *280* (1–2), 762–770.

(24) Belfer, S.; Purinson, Y.; Fainshtein, R.; Radchenko, Y.; Kedem, O. Surface modification of commercial composite polyamide reverse osmosis membranes. *J. Membr. Sci.* **1998**, *139* (2), 175−181.
(25) Van Wagner, E. M.; Sagle, A. C.; Sharma, M. M.; La, Y. H.; Freeman, B. D. Surface modification of commercial polyamide desalination membranes using poly(ethylene glycol) diglycidyl ether to enhance membrane fouling resistance. *J. Membr. Sci.* **2011**, *367* (1−2), 273−287.
(26) Kang, G. D.; Liu, M.; Lin, B.; Cao, Y. M.; Yuan, Q. A novel method of surface modification on thin-film composite reverse osmosis membrane by grafting poly(ethylene glycol). *Polymer* **2007**, *48* (5), 1165−1170.
(27) Kang, G. D.; Yu, H. J.; Liu, Z. N.; Cao, Y. M. Surface modification of a commercial thin film composite polyamide reverse osmosis membrane by carbodiimide-induced grafting with poly-(ethylene glycol) derivatives. *Desalination* **2011**, *275* (1−3), 252−259.
(28) Zou, L.; Vidalis, I.; Steele, D.; Michelmore, A.; Low, S. P.; Verberk, J. Q. J. C. Surface hydrophilic modification of RO membranes by plasma polymerization for low organic fouling. *J. Membr. Sci.* **2011**, *369* (1−2), 420−428.
(29) Jeon, S. I.; Lee, J. H.; Andrade, J. D.; Degennes, P. G. Protein surface interactions in the presence of polyethylene oxide 0.1. simplified theory. *J. Colloid Interface Sci.* **1991**, *142* (1), 149−158.
(30) Mi, B.; Elimelech, M. Chemical and physical aspects of organic fouling of forward osmosis membranes. *J. Membr. Sci.* **2008**, *320* (1−2), 292−302.
(31) Mi, B. X.; Elimelech, M. Organic fouling of forward osmosis membranes: Fouling reversibility and cleaning without chemical reagents. *J. Membr. Sci.* **2010**, *348* (1−2), 337−345.
(32) Tang, C. Y.; She, Q.; Lay, W. C. L.; Wang, R.; Fane, A. G. Coupled effects of internal concentration polarization and fouling on flux behavior of forward osmosis membranes during humic acid filtration. *J. Membr. Sci.* **2010**, *354* (1−2), 123−133.
(33) Valladares Linares, R.; Yangali-Quintanilla, V.; Li, Z.; Amy, G. NOM and TEP fouling of a forward osmosis (FO) membrane: Foulant identification and cleaning. *J. Membr. Sci.* **2012**, *421−422*, 217−224.
(34) Liu, Y. L.; Mi, B. X. Combined fouling of forward osmosis membranes: Synergistic foulant interaction and direct observation of fouling layer formation. *J. Membr. Sci.* **2012**, *407*, 136−144.
(35) Tiraferri, A.; Kang, Y.; Giannelis, E. P.; Elimelech, M. Highly hydrophilic thin-film composite forward osmosis membranes function-alized with surface-tailored nanoparticles. *ACS Appl. Mater. Interfaces* **2012**, *4* (9), 5044−5053.
(36) Tiraferri, A.; Kang, Y.; Giannelis, E. P.; Elimelech, M. Superhydrophilic thin-film composite forward osmosis membranes for organic fouling control: fouling behavior and antifouling mechanisms. *Environ. Sci. Technol.* **2012**, *46* (20), 11135−44.
(37) Ang, W. S.; Elimelech, M. Protein (BSA) fouling of reverse osmosis membranes: Implications for wastewater reclamation. *J. Membr. Sci.* **2007**, *296* (1−2), 83−92.
(38) McCutcheon, J. R.; Elimelech, M. Influence of concentrative and dilutive internal concentration polarization on flux behavior in forward osmosis. *J. Membr. Sci.* **2006**, *284* (1−2), 237−247.
(39) Ben-Asher, J. Irrigation with saline water. *GeoJournal* **1987**, *15* (3), 267−272.
(40) Li, Q.; Elimelech, M. Organic Fouling and Chemical Cleaning of Nanofiltration Membranes: Measurements and Mechanisms. *Environ. Sci. Technol.* **2004**, *38* (17), 4683−4693.
(41) Senden, T. J. Force microscopy and surface interactions. *Curr. Opin. Colloid Interface Sci.* **2001**, *6* (2), 95−101.
(42) Han, J. T.; Lee, D. H.; Ryu, C. Y.; Cho, K. W. Fabrication of superhydrophobic surface from a supramolecular organosilane with quadruple hydrogen bonding. *J. Am. Chem. Soc.* **2004**, *126* (15), 4796−4797.
(43) van Oss, C. J.; Giese, R. F.; Docoslis, A. Hyperhydrophobicity of the water−air interface. *J. Disp. Sci. Technol.* **2005**, *26* (5), 585−590.
(44) Ellison, A. H.; Zisman, W. A. Wettability of halogenated organic solid surfaces. *J. Phys. Chem.* **1954**, *58* (3), 260−265.
(45) Park, Y. S.; Won, J.; Kang, Y. S. Preparation of poly(ethylene glycol) brushes on polysulfone membranes for olefin/paraffin separation. *Langmuir* **2000**, *16* (24), 9662−9665.
(46) Belfer, S.; Purinson, Y.; Kedem, O. Surface modification of commercial polyamide reverse osmosis membranes by radical grafting: An ATR-FTIR study. *Acta Polym.* **1998**, *49* (10−11), 574−582.
(47) Bernstein, R.; Beller, S.; Freger, V. Surface modification of dense membranes using radical graft polymerization enhanced by monomer filtration. *Langmuir* **2010**, *26* (14), 12358−12365.
(48) Bernstein, R.; Belfer, S.; Freger, V. Toward improved boron removal in RO by membrane modification: Feasibility and challenges. *Environ. Sci. Technol.* **2011**, *45* (8), 3613−3620.
(49) Lee, H.; de Vries, A. H.; Marrink, S. J.; Pastor, R. W. A coarse-grained model for polyethylene oxide and polyethylene glycol: Conformation and hydrodynamics. *J. Phys. Chem. B* **2009**, *113* (40), 13186−13194.
(50) Kulkarni, A. M.; Chatterjee, A. P.; Schweizer, K. S.; Zukoski, C. F. Effects of polyethylene glycol on protein interactions. *J. Chem. Phys.* **2000**, *113* (21), 9863−9873.
(51) Tang, C. Y. Y.; Kwon, Y. N.; Leckie, J. O. Probing the nano- and micro-scales of reverse osmosis membranes—A comprehensive characterization of physiochemical properties of uncoated and coated membranes by XPS, TEM, ATR-FTIR, and streaming potential measurements. *J. Membr. Sci.* **2007**, *287* (1), 146−156.
(52) Petersen, R. J. Composite reverse-osmosis and nanofiltration membranes. *J. Membr. Sci.* **1993**, *83* (1), 81−150.
(53) Elimelech, M.; Chen, W. H.; Waypa, J. J. Measuring the zeta (electrokinetic) potential of reverse-osmosis membranes by a streaming potential analyzer. *Desalination* **1994**, *95* (3), 269−286.
(54) Coronell, O.; Marinas, B. J.; Zhang, X. J.; Cahill, D. G. Quantification of functional groups and modeling of their ionization behavior in the active layer of FT30 reverse osmosis membrane. *Environ. Sci. Technol.* **2008**, *42* (14), 5260−5266.
(55) Abiman, P.; Wildgoose, G. G.; Crossley, A.; Jones, J. H.; Compton, R. G. Contrasting pK(a) of protonated bis(3-aminopropyl)-terminated polyethylene glycol "Jeffamine" and the associated thermodynamic parameters in solution and covalently attached to graphite surfaces. *Chem.-A Eur. J.* **2007**, *13* (34), 9663−9667.
(56) Freger, V.; Gilron, J.; Belfer, S. TFC polyamide membranes modified by grafting of hydrophilic polymers: An FT-IR/AFM/TEM study. *J. Membr. Sci.* **2002**, *209* (1), 283−292.
(57) Giepmans, B. N. G.; Adams, S. R.; Ellisman, M. H.; Tsien, R. Y. Review—The fluorescent toolbox for assessing protein location and function. *Science* **2006**, *312* (5771), 217−224.
(58) Geise, G. M.; Lee, H. S.; Miller, D. J.; Freeman, B. D.; Mcgrath, J. E.; Paul, D. R. Water purification by membranes: The Role of Polymer Science. *J. Polym. Sci., Part B: Polym. Phys.* **2010**, *48* (15), 1685−1718.
(59) McCloskey, B. D.; Park, H. B.; Ju, H.; Rowe, B. W.; Miller, D. J.; Chun, B. J.; Kin, K.; Freeman, B. D. Influence of polydopamine deposition conditions on pure water flux and foulant adhesion resistance of reverse osmosis, ultrafiltration, and microfiltration membranes. *Polymer* **2010**, *51* (15), 3472−3485.
(60) Fonseca, A. C.; Summers, R. S.; Greenberg, A. R.; Hernandez, M. T. Extra-cellular polysaccharides, soluble microbial products, and natural organic matter impact on nanofiltration membranes flux decline. *Environ. Sci. Technol.* **2007**, *41* (7), 2491−2497.
(61) Herzberg, M.; Kang, S.; Elimelech, M. Role of extracellular polymeric substances (EPS) in biofouling of reverse osmosis membranes. *Environ. Sci. Technol.* **2009**, *43* (12), 4393−4398.
(62) Ang, W. S.; Yip, N. Y.; Tiraferri, A.; Elimelech, M. Chemical cleaning of RO membranes fouled by wastewater effluent: Achieving higher efficiency with dual-step cleaning. *J. Membr. Sci.* **2011**, *382* (1−2), 100−106.
(63) Hoek, E. M. V.; Elimelech, M. Cake-enhanced concentration polarization: A new fouling mechanism for salt-rejecting membranes. *Environ. Sci. Technol.* **2003**, *37* (24), 5581−5588.

(64) Lee, S.; Boo, C.; Elimelech, M.; Hong, S. Comparison of fouling behavior in forward osmosis (FO) and reverse osmosis (RO). *J. Membr. Sci.* **2010**, *365* (1−2), 34−39.
(65) Ramon, G. Z.; Hoek, E. M. V. Transport through composite membranes, part 2: Impacts of roughness on permeability and fouling. *J. Membr. Sci.* **2013**, *425*−*426*, 141−148.
(66) Israelachvili, J. N., *Intermolecular and Surface Forces*, 3rd ed.; Academic Press: Burlington, MA, 2011; p 215.